CLASSIFYING AYURVEDIC PULSE SIGNALS VIA CONSENSUS LOCALLY LINEAR EMBEDDING

Amod Jog, Aniruddha Joshi, Sharat Chandran
Dept. of Computer Science and Engineering, Indian Institute of Technology Bombay, Powai, Mumbai- 400076, India

Anant Madabhushi
Dept. of Biomedical Engineering, Rutgers University, Piscataway, NJ 08854, U.S.A.

Keywords: Pulse diagnosis, Nonlinear dimensionality reduction, Time series analysis, C-LLE, LLE, Isomap, Mutual information, Relative entropy.

Abstract: In this paper, we present a novel method for analysis of Ayurvedic pulse signals via a recently developed nonlinear dimensionality reduction scheme called Consensus Locally Linear Embedding (C-LLE). Pulse Based Diagnosis (PBD) is a prominent method of disease detection in Ayurveda, the system of Indian traditional medicine. Ample anecdotal evidence suggests that for several conditions, PBD, based on sensing changes in the patient's pulse waveform, is superior to conventional allopathic diagnostic methods. PBD is an inexpensive, non-invasive, and painless method; however, a lack of quantification and standardization in Ayurveda, and a paucity of expert practitioners, has limited its widespread use. The goal of this work is to develop the first Computer-Aided Diagnosis (CAD) system able to distinguish between normal and diseased patients based on their PBD. Such a system would be inexpensive, reproducible, and facilitate the spread of Ayurvedic methods. Digitized Ayurvedic pulse signals are acquired from patients using a specialized pulse waveform recording device. In our experiments we considered a total of 50 patients. The 50 patients comprised of two cohorts obtained at different frequencies. The first cohort comprised 24 patients that were normal or diseased (slipped disc (backache), stomach ailments) while the second consists of a set of 26 patients who were normal or diseased (diabetic, with skin disorders, slipped disc (backache) and stress related headaches). In this study, we consider the C-LLE scheme which non-linearly projects the high-dimensional Ayurvedic pulse data into a lower dimensional space where a consensus clustering scheme is employed to distinguish normal and abnormal waveforms. C-LLE differs from other linear and nonlinear dimensionality reduction schemes in that it respects the underlying nonlinear manifold structure on which the data lies and attempts to directly estimate the pairwise object adjacencies in the lower dimensional embedding space. A major contribution of this work is that it employs non-Euclidean similarity measures such as mutual information and relative entropy to estimate object similarity in the high-dimensional space which are more appropriate for measuring the similarity of the pulse signals. Our C-LLE based CAD scheme results in a classification accuracy of 80.57% using relative entropy as the signal distance measure in distinguishing between normal and diseased patients for the first cohort, based on their Ayurvedic pulse signal. For the 500Hz data we got a maximum of 88.34% accuracy with C-LLE and relative entropy as a distance measure. Furthermore, C-LLE was found to outperform LLE, Isomap, PCA across multiple distance measures for both cohorts.

1 INTRODUCTION

Diagnosis of bodily disorders by the analysis of the arterial pulse techniques has been practised in Ayurveda, a system of traditional Indian medicine. It is believed that the functioning of the human body is governed by three humors, *vata*, *pitta* and *kapha*, together known as *Tridosha*. The *Tridosha* is analyzed by obtaining the pulse waveform observed at the three positions on the wrist. The imbalances in *Tridosha* pressure waveforms are sensed by the practitioner who then identifies the presence and location of the disorders in the body (Lad, 2005). Anecdotal evidence strongly suggests that traditional Ayurvedic pulse diagnosis is able to identify certain ailments, such as stomach disorders and maladies in some preg-

Jog A., Joshi A., Chandran S. and Madabhushi A. (2009).
CLASSIFYING AYURVEDIC PULSE SIGNALS VIA CONSENSUS LOCALLY LINEAR EMBEDDING.
In *Proceedings of the International Conference on Bio-inspired Systems and Signal Processing*, pages 388-395
DOI: 10.5220/0001554903880395

nant women, more easily compared to conventional allopathic techniques. Pulse based diagnosis also has the advantage of being inexpensive, non-invasive, and painless. The practitioners 'feel' for a certain pattern in the pulse which forms the basis of their diagnosis. This technique requires a high degree of expertise. The paucity of expert Ayurvedic practitioners has limited the more widespread use and popularity of the Ayurvedic technique.

The goal of this work is to develop a computer aided diagnosis (CAD) system for the automated, reproducible analysis of Ayurvedic pulse signals. To the best of our knowledge, this work represents the first attempt at CAD of Ayurvedic pulse signals.

Since the Ayurvedic pulse signal is a time series, pattern recognition methods that have been previously applied to analysis of other time series data (ECG, EMG) might seem appropriate for CAD of PBD. Pattern recognition in electrocardiogram (ECG) has been applied to QRS/PVC recognition and classification, the recognition of ischemic beats and episodes, and the detection of atrial fibrillation using nonlinear transformations and neural networks (Maglaveras et al., 1998). In (Maglaveras et al., 1998), a model-based approach for classification of ECG studies based on previously defined signatures of normal and diseased ECG signals was employed. Given that this is a first CAD attempt at Ayurvedic PBD, quantitative signatures for normal and diseased patterns have yet to be studied and modelled. We consequently explore a domain independent scheme for classification of the pulse data via dimensionality reduction.

Dimensionality reduction (DR), is a transformation of the original high-dimensional feature space to a space of eigenvectors which are capable of describing the data in far fewer dimensions. DR also permits the visualization of individual data classes and identification of possible subclasses within the high dimensional data. The most popular method for DR is Principal Component Analysis (PCA) which attempts to find orthogonal eigenvectors accounting for the greatest amount of variability in the data. PCA assumes that the data is linear and the embedded eigenvectors represent low-dimensional projections of linear relationships between data points in high-dimensional space. However, our previous research has strongly suggested that biomedical data is highly nonlinear in nature (Lee et al., 2008) and that nonlinear DR schemes such as Isometric Mapping (Isomap) (Tenenbaum et al., 2000), Locally Linear Embedding (LLE), (Roweis and Saul, 2000) are more appropriate for projection and subsequent classification of high-dimensional data including protein, gene-expression, and spectroscopic data. LLE and Isomap assume that the high dimensional data on a high-order curve that is highly nonlinear and hence object distances measured on this nonlinear manifold should be geodesic as opposed to Euclidean. Nonlinear methods attempt to map data along this nonlinear manifold by assuming only neighboring points (determined via geodesic proximity) to be similar enough to be mapped linearly with minimal error. The nonlinear manifold can then be reconstructed based on these locally linear assumptions.

NLDR schemes like LLE determine the neighboring locations on the manifold (via Euclidean distance) and map the neighborhood associated with each object into the reduced dimensional embedding space. The size of the local neighborhood within which LLE assumes local linearity is however determined by a free parameter κ. Optimal estimation of κ is still an open problem. In (Tiwari et al., 2008) a new NLDR scheme, C-LLE, that is able to handle the limitations of LLE by avoiding the κ estimation, focusing instead on optimally determining pairwise object distances in the low dimensional embedding space, was presented.

Another limitation of LLE is that it traditionally employs the Euclidean distance measure to determine neighbors within local patches on the manifold. While the Euclidean distance measure is appropriate for measuring the distance between objects characterized by discrete attributes, it is less appropriate for measuring pulse signal similarity. Non-Euclidean distance measures such as mutual information (MI), entropy correlation coefficient (ECC), and the relative entropy (RE) have been shown to be more appropriate for measuring the similarity between signals compared to the L2 norm (Tononi et al., 1996). In this paper, the C-LLE algorithm is employed in conjunction with such signal similarity measures as MI, ECC, and RE to embed Ayurvedic pulse signals in a lower-dimensional embedding space. Prior to embedding, the pulse signals are first aligned with respect to each other so that the pulse peaks for the different studies are in concordance. A consensus clustering (Strehl and Ghosh, 2002) algorithm is then employed to discriminate between the normal and diseased pulse signals in the lower dimensional embedding space. The major contributions of this work are:

- To the best of our knowledge, this is the first CAD system for classification and analysis of traditional Indian Ayurvedic pulse medicine.
- Our CAD approach employs the C-LLE algorithm that we have previously shown to outperform LLE, Isomap.
- We introduce the use of non-Euclidean distance measures (MI, ECC, RE) geared specifically to determining signal similarity for identifying

neighbors in the high dimensional space. Our hypothesis is that the use of these distance measures will result in a more meaningful, accurate low dimensional embedding for pulse signal data.

The remainder of the paper is organized as follows. Section 2 gives a brief review of dimensionality reduction methods used and the motivation for C-LLE. Section 3 provides an overview of the CAD system. Section 4 describes our experimental design and gives a detailed description of C-LLE. In Section 5 we present the qualitative and quantitative results of our CAD system and concluding remarks, future directions are presented in Section 6

2 CONSENSUS LOCALLY LINEAR EMBEDDING (C-LLE)

2.1 Limitations of Nonlinear Dimensionality Reduction (NLDR) Methods

NLDR schemes such as LLE (Roweis and Saul, 2000) and Isomap (Tenenbaum et al., 2000) assume that an object in high-dimensional space can be described by linear relationships with its nearest neighbors. Both LLE and Isomap attempt to map objects $c,d \in S$ that are adjacent (via geodesic distance) in high-dimensional space to nearby points in the low-dimensional embedding, $P(c),P(d)$, where $P(c),P(d)$ represent the Eigenvectors associated with $c,d \in S$. LLE attempts to solve this problem by defining a locally linear neighborhood for each $c \in S$, the size of the neighborhood being determined by κ, parameter controlling the size of the neighborhood within which local linearity is assumed. LLE then attempts to non-linearly project each c to $P(c)$ so that the κ neighborhood of $c \in S$ is preserved. While Roweis and Saul (Roweis and Saul, 2000) have suggested that the lower dimensional embeddings are greatly robust to κ values, our own experiments have indicated otherwise (Lee et al., 2008). Note that, Roweis and Saul's experiments were performed on dense, synthetic datasets that are very different from highly noisy, nonlinear real world datasets considered in this work. It is our contention that in general it is not possible to find a global κ value that optimally fits all parts of the high-dimensional data.

2.2 Motivation for Consensus Locally Linear Embedding

One of the solutions to enable for LLE to work optimally and generally on real world data, κ needs to be locally estimated in different regions in the data space. While some researchers have recently begun to explore approaches to locally and adaptively estimate κ, (Tong and Zha, 2008) (Wang et al., 2004), the C-LLE scheme aims to estimate the pair-wise object adjacency $\hat{W}(i,j)$ in the low dimensional embedding between two objects $c_i, c_j \in S$, where $i,j \in \{1,\cdots,|S|\}$. We formulate the problem of estimating object distances $\hat{W}(i,j)$ as a Maximum Likelihood Estimation problem (MLE) from multiple approximations $W_\kappa(i,j)$ obtained by varying κ. The spirit behind C-LLE is that it combines multiple low dimensional data representations obtained via LLE for different κ values to provide a stable embedding representing the true class relationship between objects in the high dimensional space. Analogous to constructing Bagging classifier ensembles (Breiman, 1996), the idea behind C-LLE is to combine multiple weak embeddings so that the strong final embedding accurately reflects low-dimensional relationships. In addition, C-LLE allows for incorporation of non-Euclidean similarity measures in the original pulse space. Our contention is that these pulse signal similarity measures are more appropriate compared to the L2 norm. In (Tiwari et al., 2008), the utility of C-LLE in identifying and classifying prostate cancer using the Magnetic Resonance Spectroscopic Imaging (MRSI) data was demonstrated.

3 SYSTEM OVERVIEW

Our CAD system for Ayurvedic pulse signal classification (Figure 1) involves obtaining the Ayurvedic pulse signals in digital form, after which they are noise filtered and baseline corrected. The pulse signals are aligned with respect to each other based on their peaks. The aligned pulse data is embedded in a lower dimensional sub-space via C-LLE. The signals, in their reduced low-dimensional representation, are then classified into distinct classes via consensus k-means clustering (Strehl and Ghosh, 2002).

Data Description. The two cohorts of 24 and 26 Ayurvedic pulse signals acquired at different frequencies are briefly described in Table 1. The data was collected by a pulse waveform acquiring device (Joshi et al., 2007) that records the pressure felt by the sensors at three different points. Although the device

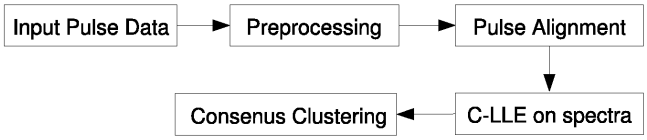

Figure 1: Flow diagram showing the different components of our C-LLE based Ayurvedic pulse diagnosis CAD system.

records all three pulse waveforms, we have used only the *Vata* pulse for the purposes of this investigation. The true condition for each patient was determined by an expert Ayurvedic pulse practitioner.

Table 1: Description of patient database.

Condition	Frequency	No. of samples
Normal	100	10
Slipped disk	100	8
Stomach ailment	100	6
Normal	500	4
Diabetes	500	7
Slipped disk	500	5
Headaches	500	3
Stomach ailments	500	7

4 EXPERIMENTAL DESIGN

4.1 Pre-processing

For each patient study $c \in S$, there is an associated D-dimensional valued pulse vector $\mathbf{F}(c) = [f_t(c) \mid t \in \{1, \cdots, D\}]$ where $f_t(c)$ is the scalar pressure intensity recorded at every instant. We denote via $\Delta = \{\text{LLE}, \text{Isomap}, \text{C-LLE}\}$ the set of dimensionality reduction techniques considered in this paper. For each study c and associated pulse vector $\mathbf{F}(c)$, initial preprocessing involves the following:

1. Respiration and artifact motion during pulse waveform acquisition can introduce baseline wander, which can be removed via the adaptive baseline wander removal method described in (Xu et al., 2002).
2. Each time series $\mathbf{F}(c)$ is filtered to remove high frequency noise via a soft thresholding wavelet scheme (Novak et al., 2000).
3. Each of the signals $\mathbf{F}(c)$, $c \in S$, is then centered on the mean and normalized. Figure 2 shows a pulse signal $\mathbf{F}(u)$ (a) prior to and (b) following noise and baseline correction and pulse signal normalization.

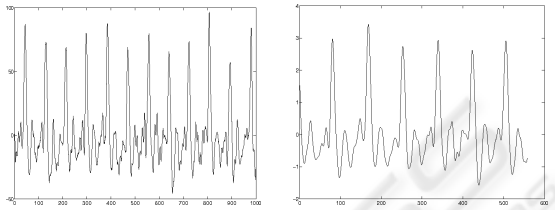

(a) (b)

Figure 2: The pulse signal (a) prior to and (b) following noise and baseline correction and pulse signal normalization.

4.2 Pulse Signal Alignment

Pulse signal alignment is a necessary prerequisite to computing similarity between data points and identifying neighbors in the high-dimensional pulse signal space. For instance, if the Euclidean metric is employed to measure pulse signal similarity, an offset of even a single time point can result in an incorrect distance value.

Each time-signal $\mathbf{F}(c)$ is characterized by a certain periodic pattern of peaks. A simple peak detection algorithm (Billauer, 2004) was used to find the dominant peaks in $\mathbf{F}(c)$, $\forall c \in S$. The first occurrence of a dominant peak in $\mathbf{F}(c)$ was identified on all $c \in S$ which were then aligned with respect to each other. Note that while additional anchor points (additional modes) could also have been used for the pulse signal alignment, Figure 3(b) suggests that a single anchor point (in this case the first dominant peak) resulted in reasonable alignment. The pulse signal alignment method is analogous to an intensity standardization scheme that we previously presented (Madabhushi and Udupa, 2005) to correct for nonlinear intensity artifacts in MRI. Figure 3 shows the different signals (a) prior to and (b) following alignment.

4.3 Similarity Measures

LLE, Isomap identify object neighbors as those that are in proximity of each other in terms of the Euclidean distance metric. The L2 norm is not however optimally suited for measuring pulse signal similarity. Consequently we consider several non-Euclidean metrics (described in sections 4.3.1 - 4.3.4) that are more appropriate for measuring signal similarity.

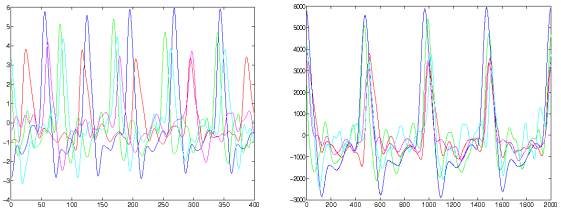

(a) (b)

Figure 3: Five pulse signals superimposed (a) before and (b) after pulse signal alignment. Notice that the signals are more aligned.

4.3.1 Euclidean Distance

Consider the two pulse signal vectors $\mathbf{F}(c)$ and $\mathbf{F}(d)$ for $c,d \in S$. The Euclidean distance between them is defined as

$$\Gamma^{Eu}(c,d) = \sqrt{\sum_t (f_t(c) - f_t(d))^2} \qquad (1)$$

where $t \in \{1,...,D\}$. The Euclidean distance metric requires the existence of an orthogonal coordinate system. Since the individual components of $\mathbf{F}(c)$ ($f_t(c), t \in \{1,\cdots,D\}$) do not constitute an orthogonal basis, Euclidean distance is perhaps a sub-optimal measure for determining signal similarity.

4.3.2 Normalized Mutual Information

In information theory, the Shannon entropy or information entropy is a measure of the uncertainty associated with a random variable. The vector of values $\mathbf{F}(c)$, associated with a signal takes can be thought of as a random variable. From a signal we can derive the probability distribution of these values. These probability distributions $p(x_i)$ are used to define the information entropy of a discrete random variable $X = \{x_1,\cdots,x_n\}$ as,

$$H(X) = -\sum_{i=1}^{n} p(x_i)\log p(x_i) \qquad (2)$$

Considering two random variables X and Y, their joint entropy is defined to be

$$H(X,Y) = -\sum_{x,y} p_{x,y}\log p_{x,y} \qquad (3)$$

where $p_{x,y}$ is the probability density function for the joint distribution of X and Y. The mutual information (*MI*) between these two random variables is defined to be

$$I(X,Y) = H(X) + H(Y) - H(X,Y) \qquad (4)$$

MI measures the dependence of one variable on the other which is a similarity measure, is used widely in medical image registration (Pluim et al., 2003). A normalized variant of *MI* is defined as follows (Pluim et al., 2003).

$$NMI(X,Y) = \frac{H(X)+H(Y)}{H(X,Y)} \qquad (5)$$

When the two variables X and Y are completely identical, $NMI(X,Y) = 2$. Thus, we define the distance metric $\Gamma^{NMI} = 2 - NMI$.

4.3.3 Entropy Correlation Coefficient (*ECC*)

Another measure which can be directly calculated from the entropy values is the Entropy Correlation Coefficient (*ECC*) and is defined as follows (Pluim et al., 2003):

$$ECC(X,Y) = 2 - \frac{2H(X,Y)}{(H(X)+H(Y))} \qquad (6)$$

Therefore, $ECC = 1$ if the two distributions are identical and $ECC = 0$ if they are completely independent. This allows us to define the distance metric $\Gamma^{ECC} = 1 - ECC$.

4.3.4 Relative Entropy

Relative Entropy (*RE*), or the Kullback-Leibler Distance (Cover and Thomas, 1991), used for measuring the distance between probability distributions is defined as follows:

$$RE(X,Y) = \sum_i p(x_i)\log\frac{p(x_i)}{p(y_i)} \qquad (7)$$

or in other words

$$RE(X,Y) = C(X,Y) - H(X) \qquad (8)$$

where $C(X,Y)$ is defined as the cross entropy of the two variables. Note that while the Euclidean, *MI*, and *ECC* measures are both symmetric and reflexive, the *RE* measure is only reflexive.

4.4 Consensus Locally Linear Embedding Framework

The spirit behind C-LLE is that it combines multiple low-dimensional data representations obtained via LLE for different κ values to provide a stable embedding representing the true class relationship between objects in the high dimensional space. Analogous to constructing Bagging classifier ensembles (Breiman, 1996), the idea behind C-LLE is to combine multiple weak embeddings so that the strong final embedding accurately reflects low-dimensional relationships.

Step 1. Generating multiple lower dimensional embeddings by varying the parameter κ:
We generate a set of multiple embeddings $S_\kappa(c)$ for $c \in S$, by varying the neighborhood parameter $\kappa \in \{2,\ldots,K\}$ using LLE. The distance between any two objects $c_i, c_j \in S$ and $i, j \in \{1,\ldots,|S|\}$ is a function of κ. Thus $||S_\kappa(c_i) - S_\kappa(c_j)||_\psi$ will vary as a function of κ, where ψ is the distance measure.

Step 2. Obtain MLE of pairwise object adjacency:
A confusion matrix $W_\kappa \in \Re^{|S|\times|S|}$ representing the adjacency between any two time series $c_i, c_j \in S$ and $i, j \in \{1,\ldots,|S|\}$ in the lower dimensional embedding $S_\kappa(c)$ is calculated as:

$$W_\kappa(i,j) = \mathcal{D}_\kappa(c_i,c_j) = \left\|S_\kappa(c_i) - S_\kappa(c_j)\right\|_\psi, \quad (9)$$

where $\kappa \in \{2,\cdots,K\}$. MLE of $\mathcal{D}_\kappa(c_i,c_j)$ is estimated as the mode of all adjacency values in $\hat{\mathcal{D}}_\kappa(i,j)$ over all κ. This $\hat{\mathcal{D}}$ for all $c \in S$ is then used to obtain the new confusion matrix $\hat{W}$.

Step 3. Multidimensional scaling (MDS):
We apply multidimensional scaling (Venna and Kaski, 2006) (MDS) to $\hat{W}$ to achieve the final stable embedding $\tilde{S}(c)$, for all $c \in C$. MDS is implemented as a linear method that preserves the Euclidean geometry between each pair of objects $c_i, c_j \in S$, i, $j \in \{1,...,|S|\}$. This is done by finding optimal positions for the data points c_i, c_j in lower-dimensional space through minimization of the least squares error in the input pairwise Euclidean distances in $\hat{W}$. After the application of LLE in Step:1, we have essentially embedded the points in a linear subspace, where the L2 norm is appropriate.

4.5 Consensus k-means Clustering on the Embedding

Let Q be the set of all low dimensions we are ranging over for embedding. The output of MDS is an embedding location $\tilde{S}(c)$, $\forall c \in S$ which spans $Q \in \{3,\cdots,15\}$. This set can be represented by a $|S| \times q$ matrix where each row is an embedding in q dimensional space of the original point in q dimensions where $q \in Q$. The next step on acquiring the embedding in lower dimensions is to group all $c \in S$ points into two clusters (normal and abnormal). For the first cohort consisting of 100Hz data, we are grouping the points into normal and abnormal cluster. This grouping is done using consensus k-means clustering algorithm (Strehl and Ghosh, 2002). To overcome the instability associated with centroid based clustering algorithms like k-means clustering, we generate multiple weak clusterings V_a^1 , V_a^2, $a \in \{1,\ldots A\}$ by repeated application of k-means clustering on $\tilde{S}(c)$, $\forall c \in S$, a total of A times. Each cluster is a set of objects assigned the same label V_a^1 , V_a^2, by the k-means algorithm. As the number of objects in a cluster keep on changing, we calculate a co-association matrix H with the assumption that points belonging to a *natural* cluster are very likely to be co-located in the same cluster for each iteration a. Co-occurrences of pairs of points $c_i, c_j \in S$ are taken as *votes* for their association. $H(i,j)$ thus is the number of times c_i and c_j were found in the same cluster over A iterations. If $H(i,j) = A$, it is highly likely that c_i and c_j belong to the same cluster. MDS to H followed by a final unsupervised classification using k-means clustering is used to obtain the final stable clusters $\tilde{V}^1$ and $\tilde{V}^2$.

5 RESULTS

5.1 Qualitative Results

Figure 4 (a) (d) show the low-dimensional embedding representation of the 100Hz and 500Hz data respectively obtained via C-LLE. Figures 4 (b) (c) show the corresponding embedding results obtained with LLE and PCA for the 100Hz cohort and figures 4 (e) (f) for LLE and Isomap embeddings the 500Hz data. In each case, the blue squares represent the normal studies and red stars represent diseased cases. The embedding results in Figures 4(a)-(c) were all obtained by projecting the aligned pulse data into 3 dimensions via the relative entropy similarity measure. In comparing Figures 4(a)-(c), and Figures 4 (d)-(f) it is apparent that the greatest separation between the normal and diseased studies is obtained via C-LLE. LLE performs marginally better compared to PCA in terms of separating the pulse signals, reinforcing further that NLDR schemes outperform linear DR schemes for biomedical data.

5.2 Quantitative Results

In order to quantitatively evaluate the different approaches, the following experiments were performed: (a) C-LLE was compared against other NLDR methods (LLE, Isomap) in terms of classification accuracy and for different similarity measures (b) the effect of pulse signal alignment of the data on the results of NLDR was analyzed for the 100Hz signal. For the 500Hz signal we compare the performance of C-LLE over different similarity measures.

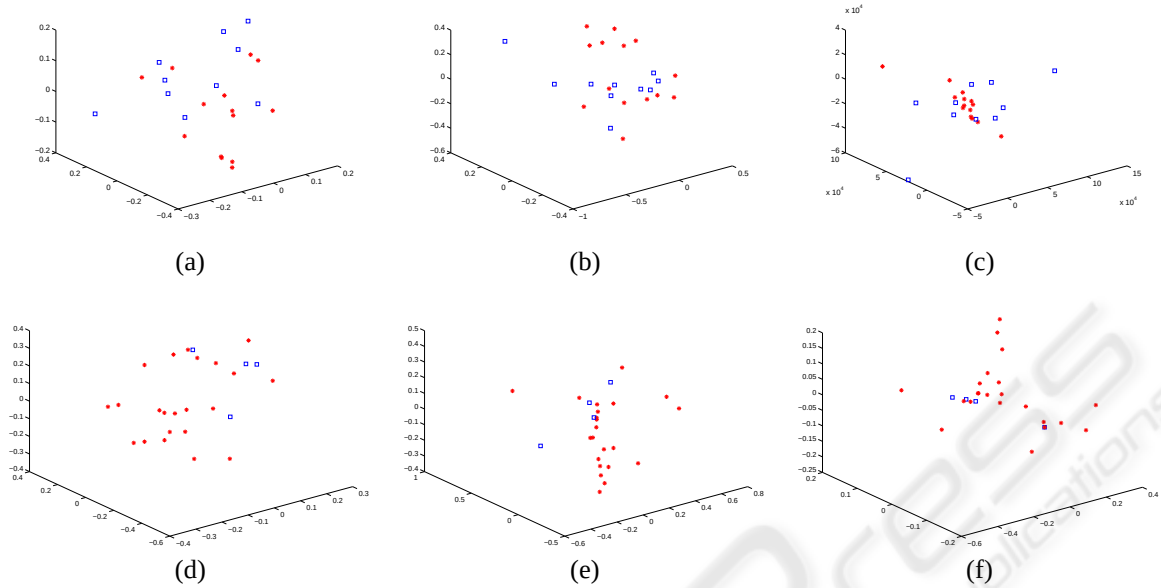

Figure 4: Low-dimensional embedding of 100Hz pulse data obtained via (a) C-LLE, (b) LLE, and (c) PCA after alignment, and the same for 500Hz data using (d) C-LLE, (e) LLE (f) Isomap. The red asterisks represent diseased pulse samples whereas the blue squares represent normal.

5.2.1 Comparison of C-LLE with other DR Methods for Different Similarity Measures

We compare the classification accuracy as obtained by C-LLE with LLE and Isomap over the 4 similarity measures Γ^{Eu}, Γ^{NMI}, Γ^{ECC} and Γ^{Re}. Table 2 clearly indicates that C-LLE achieves a higher classification accuracy than LLE and Isomap for all 4 similarity measures for the 100Hz cohort normal vs abnormal classification. C-LLE with Γ^{Re} as the similarity measure yields a classification accuracy of 80.57%, significantly higher compared to LLE and Isomap. With the exception of Γ^{Eu}, all C-LLE results are over 70%. The classification accuracy for Γ^{Eu} is the lowest among all similarity measures for all the 3 methods.

Table 2: Classification accuracy in (%) of DR methods for 100Hz data for normal vs abnormal classification after pulse alignment.

$\Delta\|\Gamma$	Γ^{Re}	Γ^{NMI}	Γ^{ECC}	Γ^{Eu}
C-LLE	**80.57**	**72.20**	**70.83**	60.08
LLE	64.16	60.83	61.67	41.66
Isomap	46.36	21.00	58.82	48.67

For the 500Hz signal, we obtained the following results for C-LLE across 3 similarity measures. We observe that Γ_{Re} provides the highest accuracy of classification of 88.34%.

Table 3: Classification accuracy (in %) of C-LLE for 500Hz data for normal vs abnormal classification.

$\Delta\|\Gamma$	Γ^{Re}	Γ^{NMI}	Γ^{Eu}
C-LLE	**88.34**	71.15	76.92

5.2.2 Effect of Pulse Signal Alignment on Classification Accuracy of C-LLE and LLE over 4 Different Similarity Measures

Table 4 lists the classification accuracy obtained via C-LLE and LLE over different similarity measures with and without pulse signal alignment for the 100Hz data set for normal vs abnormal classification. The columns 'w' indicate with alignment, 'w/o' is without alignment. As the results in Table 4 clearly reveal, the classification accuracy results obtained following pulse signal alignment are consistently higher compared to the results obtained without pulse signal alignment, independent of the NLDR method and similarity measure employed.

6 CONCLUDING REMARKS AND FUTURE WORK

In this paper we have presented a novel nonlinear dimensionality reduction technique (Consensus Locally

Table 4: Effect of Pulse Signal Alignment on the Classification Accuracy (in %) for the 100Hz data.

$\Delta\|\Gamma$	Γ^{Eu}		Γ^{NMI}		Γ^{Re}		Γ^{ECC}	
–	w	w/o	w	w/o	w	w/o	w	w/o
C-LLE	60.08	50.59	72.20	32.74	**80.57**	32.73	70.83	50.00
LLE	41.66	54.50	60.83	55.35	64.16	52.38	61.67	52.97
Isomap	55.35	61.16	21.00	52.97	46.36	31.67	58.82	32.91

Linear Embedding) for the classification and analysis of Ayurvedic pulse signals. To the best of our knowledge, this is the first CAD system for analysis of traditional Ayurvedic pulse signals. Another important contribution of the paper is the use of non-Euclidean similarity measures that are more appropriate for measuring pulse signal similarity. These measures (Mutual Information, Relative Entropy, and Entropy Correlation Coefficient) were all found to consistently result in better classification compared to the L2 norm, independent of the NLDR method used. Additionally, C-LLE consistently outperformed LLE and Isomap for all 4 similarity measures considered. C-LLE with relative entropy as a distance measure provided a maximum accuracy of 80.57% for the 100Hz data, and a maximum of 88.34% for the 500Hz data. In future work, we will explore in greater detail the pulse signals that were misclassified by our CAD scheme. We will also explore alternative representations of the data such as independent components and Hölder exponents for feature selection. Finally, we will be looking to evaluate our methods on a larger data cohort.

REFERENCES

Billauer, E. (2004). peakdet: Peak detection using matlab.

Breiman, L. (1996). Bagging predictors. *Machine Learning*, 24(2):123–140.

Cover, T. M. and Thomas, J. A. (1991). *Elements of Information Theory*. John Wiley & Sons, Inc.

Joshi, A., Kulkarni, A., Chandran, S., Jayaraman, V. K., and Kulkarni, B. D. (2007). Nadi tarangini: A pulse based diagnostic system. In *IEEE Engineering in Medicine and Biology Society*, pages 2207–2210.

Lad, V. (2005). Secrets of the the pulse: The ancient art of ayurvedic pulse diagnosis. *Motilal Banarasidass*.

Lee, G., Rodriguez, C., and Madabhushi, A. (2008). Investigating the efficacy of nonlinear dimensionality reduction schemes in classifying gene and protein expression studies. *IEEE/ACM Transactions on Computational Biology and Bioinformatics*, 5(3):368–384.

Madabhushi, A. and Udupa, J. (2005). Evaluating intensity standardization and inhomogeneity correction in magnetic resonance images. *IEEE Transactions on of Medical Imaging*, 24(5):561–576.

Maglaveras, N., Stamkopoulos, Diamantaras, T., C., P., and Strintzis, M. (1998). Ecg pattern recognition and classification using non-linear transformations and neural networks: A review. *International Journal of Medical Informatics*, 52(1-3):191–208.

Novak, D., Eck, C., Perez-Cortes, J. V., and Andreu-Garcia, G. (2000). Denoising electrocardiographic signals using adaptive wavelets. In *BIOSIGNAL*.

Pluim, J., Maintz, P. W., and Viergever, M. (2003). Mutual-information-based registration of medical images: A survey. *IEEE Transactions on Medical Imaging*.

Roweis, S. and Saul, L. (2000). Nonlinear dimensionality reduction by locally linear embedding. *Science, v.290*, pages 2323–2326.

Strehl, A. and Ghosh, J. (2002). Cluster ensembles – a knowledge reuse framework for combining multiple partitions. *Journal on Machine Learning Research (JMLR)*, 3:583–617.

Tenenbaum, J. B., de Silva, V., and Langford, J. C. (2000). A global geometric framework for nonlinear dimensionality reduction. *Science*.

Tiwari, P., Rosen, M., and Madabhushi, A. (2008). In *MICCAI*, volume 5242, pages 330–338.

Tong, L. and Zha, H. (2008). Riemannian manifold learning. *IEEE Transactions on Pattern Analysis and Machine Intelligence*, 30:796–809.

Tononi, G., Sporns, O., and Edelman, G. M. (1996). A complexity measure for selective matching of signals by the brain. *PNAS*, 93(8):3422–3427.

Venna, J. and Kaski, S. (2006). Local multidimensional scaling. *Neural Networks*, 19:889–899.

Wang, J., Zhang, Z., and Zha, H. (2004). Adaptive manifold learning. *NIPS*.

Xu, L., Zhang, D., and Kuanquan, W. (2002). Adaptive baseline wander removal in the pulse waveform. pages 143–148.